ORIGINAL ARTICLE

Journal Section

A model study of the effect of clustering on the last stage of drizzle formation

Deepak G. Madival[1*]

[1]Engineering Mechanics Unit, Jawaharlal Nehru Center for Advanced Scientific Research, Bangalore, Karnataka, 560064, India

Correspondence
Deepak Madival, Engineering Mechanics Unit, JNCASR, Bangalore, Karnataka, 560064, India
Email: deepakmadival@jncasr.ac.in

Funding information

In the final stage of growth, settling cloud drops become drizzle by collision and coalescence with the smaller droplets in their path. We study the impact of droplet clustering on the growth of settling collector drops by modeling it as an exponentially decaying correlation. Enhancement in collector drop growth is measured by the reduction in time needed for drizzle formation in the last stage. Effect of clustering is characterized by two dimensionless parameters $C = \delta\lambda L$ and $K = (\lambda_0 L)^{-1}$, where $\delta\lambda$ is the enhancement in the collision rate inside the clusters, L is the cluster size perceived by the settling collector drop and λ_0 is the initial collision rate. Increasing C or K reduces the time needed for drizzle formation compared to the unclustered case. We find that for $K \geq 5, C \leq 2$ even a small increase in droplet concentration inside clusters can cause a significant enhancement in the collector drop growth. Further even for low turbulence intensities (low K) significant reduction in the time for drizzle formation is achieved for moderate values of C. These findings are relevant to the debate on the intensity of clustering needed to explain rapid drizzle formation.

KEYWORDS
Cloud droplet growth, Cloud droplet clustering, Gravitational collision and coalescence, Rapid drizzle formation

1 | INTRODUCTION

Rapid initiation of drizzle in cumulus clouds is a puzzle that has attracted much research effort in the cloud-physics community and beyond. Some pertinent reviews are due to Grabowski and Wang (2013), Devenish et al. (2012), Narasimha (2012), Siebert et al. (2010), and Shaw (2003). Subsequent to nucleation, growth of a cloud drop comprises three overlapping stages. In the first stage, small droplets grow predominantly by (stochastic) condensation of ambient water vapor; it results in a broad size distribution with droplets of radii up to ~ 15 μm (Grabowski and Wang, 2013). In the second stage of growth spanning the range $\sim 15-40$ μm, droplets grow predominantly by collision and coalescences orchestrated by the intense in-cloud turbulence (characterized by large eddy Reynolds number $\sim 10^6 - 10^7$, Shaw (2003)). In the final stage, large heavy drops that interact weakly with turbulence begin to settle under gravity; they become drizzle drops exceeding ~ 100 μm radius by collecting smaller droplets lying in their path. Helped by the vigorous in-cloud turbulence, the whole growth is accomplished in about half-hour (Narasimha, 2012; Szumowski et al., 1997; Rogers and Yau, 1996). Much effort has been devoted to explaining (among other issues) how the turbulence enhances inter-droplet collision rates, with major focus on the second stage of growth.

Turbulence enhances collision rate by inducing relative velocity even between droplets of the same size. Saffman and Turner (1956) showed that the rapid growth of "small" cloud droplets (of sub-Kolmogorov size and whose Stokes number$\ll 1$; latter is the ratio of droplet response time to Kolmogorov time scale, Davidson (2007)) demands turbulence with a dissipation rate ~ 2000 cm^{2}s^{-3} which rather lies at the higher end of the dissipation rates for cumulus clouds. However Maxey (1987) showed that inertial particles in a turbulent flow leave high vorticity regions to accumulate in high strain regions, which phenomenon is now called clustering (or preferential concentration or accumulation effect); since then more mechanisms for inertial particle clustering have been proposed (Bragg et al., 2015; Elperin et al., 2015; Bec et al., 2014; Coleman and Vassilicos, 2009; Mehlig and Wilkinson, 2004), see Gustavsson and Mehlig (2016), Pumir and Wilkinson (2016), for a review. Droplet clustering further enhances the collision rate because the number density in the vicinity of a droplet is now statistically higher; the enhancement is measured either by comparison with Saffman and Turner (1956)'s formula (because droplets do not cluster when $St \to 0$ or $St \to \infty$) or by computing the radial distribution function at contact between droplets (Sundaram and Collins, 1997). Numerical, semi-analytical, and (a few) experimental studies showed that clustering at sub-Kolmogorov scale among mono-disperse particles peaks when $St \sim 1$ and the consequent enhancement in collision rate can be more than an order of magnitude over the unclustered case (Ireland et al., 2016a; Gualtieri et al., 2013; Saw et al., 2008; Ray and Collins, 2011; Ayala et al., 2008; Bec et al., 2007, 2005; Zaichik et al., 2003; Alipchenkov and Zaichik, 2003; Wang et al., 2000; Reade and Collins, 2000; Zhou et al., 1998; Sundaram and Collins, 1997). Note that the collision rates thus computed are mean or effective rates; different droplets however suffer different number of collisions over a given duration. Although these studies utilized idealized flows (homogeneous, isotropic turbulence or synthetic random flows) and were limited to lower Reynolds numbers compared to the clouds, one hopes that the results will carry over to actual clouds and therefore that the clustering must be a major cause of rapid cloud-droplet growth. Further, measurements have ascertained that the cloud droplets are indeed clustered (Larsen et al., 2018; Lehmann et al., 2007; Pinsky and Khain, 2003; Kostinski and Jameson, 2003; Kostinski and Shaw, 2001; Jameson and Kostinski, 2000).

In this article we investigate the effect of clustering on the last stage of growth, that is collisional growth of the settling cloud drops. Last-stage growth spans the widest droplet size range; more importantly, the consequences of clustering shall be more apparent in this simpler setting. Telford (1955) was the first to model

the last-stage growth as a discrete stochastic process, in which a settling "collector drop" grows in steps as it collects smaller droplets. The earlier "continuous-model" of growth (Bowen, 1950; Langmuir, 1948) assumed a continuous distribution of liquid water over space; it thus tracked the change in the average droplet size, but drizzle is initiated by the outliers that comprise the tail of the size distribution. The same insight applies to the mean collision rates computed in the aforementioned studies. Telford's approach, as well as Kostinski and Shaw (2005)'s analysis of (stochastic) duration between consecutive coalescences, revealed that the continuous-model overestimates the time for drizzle formation by a factor of $\sim 6-10$. Their analyses however assumed an unclustered distribution of smaller droplets. Here too we shall treat the collisions as a discrete stochastic process and focus on the tail of the drop size distribution (the fortunate outliers). Effect of clustering on the collision process shall be heuristically modeled by an exponentially-decaying memory or correlation function (in contrast, the collisions in an unclustered distribution is a memoryless Poisson process, Kostinski and Shaw (2005)). The rest of the article is organized as follows. In Sect. 2 we present the stochastic growth equation for the settling drops and show how the exponentially decaying memory is incorporated into it. The numerical procedure for obtaining the solution is presented in Sect. 3. In Sect. 4 the results are presented and discussed. Finally in Sect. 5 we conclude and summarize the work.

2 | STOCHASTIC GROWTH EQUATION IN THE PRESENCE OF CLUSTERING

We study the growth of a population of sparsely-distributed, therefore independently-growing, large collector drops settling under gravity inside a cloud of identical smaller droplets of volume v. Smaller droplets interact with a background turbulent flow which is assumed stationary and homogeneous. We adopt the reference frame in which the mean settling velocity of smaller droplets is zero. The number-density statistics of smaller droplets is assumed homogeneous (at least in the direction of fall) characterized by an average n_0 measured over a spatial volume large compared to that of the clusters. Our aim is to find the probability that a collector drop of initial volume V_0 beginning at z_0 (Z-axis is vertically downward) suffers k collision- and-coalescence events after falling through a distance $h = z - z_0$. This discrete conditional probability function is denoted $P(k|h, V_0)$, $k \in \{0, 1, 2, \ldots\}$. Towards that end we first define two probability functions: (1) No-collision probability function, $G(h|V)$, which gives the probability that a collector drop of volume V does not suffer a collision through a distance of fall h, and (2) First-collision probability function, $f(h|V)$, such that $f(h|V)\delta h$ gives the probability that a collector drop of volume V suffers its first collision in the δh neighborhood of distance of fall h. The two probability functions are related by (Madival, 2018):

$$f(h|V) = -\frac{d}{dh}G(h|V) \tag{1}$$

Since a collector drop cannot suffer a collision within zero distance of fall we also have $G(h = 0|V) = 1$.

After k collision-and-coalescences collector drop's volume becomes $V_k = V_0 + kv$, with the corresponding radius R_k. Let $\mathbf{L} \equiv \int_0^\infty dh\ \exp(-hs)$ denote the Laplace transform operator and define $\mathbf{G}_k(s) \equiv \mathbf{L}[G(h|V_k)], \mathbf{f}_k(s) \equiv \mathbf{L}[f(h|V_k)] = 1 - s\mathbf{G}_k(s)$. The probability that a collector drop suffers k collision-and-coalescences through a distance of fall h, which is also the probability that it grows to a volume V_k, is (see

Madival (2018) for details):

$$P(k|h,V_0) = \mathbf{L}^{-1}\left[\mathbf{G}_k \prod_{i=0}^{k-1} \mathbf{f}_i\right], \quad \mathbf{f}_i(s) = 1 - s\mathbf{G}_i(s) \tag{2}$$

where $\mathbf{L}^{-1}$ denotes the inverse Laplace transform operator. Above result assumes that the coalescence efficiency is 1, that is, every collision results in coalescence. Determining coalescence efficiency in the presence of turbulence is difficult (Vohl et al., 2007; Beard and Ochs, 1984), but for colliding drops of disparate sizes the assumption is not unreasonable. Our task now is to seek a no-collision probability function $G(h|V)$ that accounts for the droplet clustering.

We begin with the case of the unclustered distribution of smaller droplets and then generalize the argument to the clustered case. If R_k is the collector drop radius and r is the smaller droplet radius then the mean rate of collision of the collector drop per unit distance of fall, $\lambda_k = E_k n_0 \pi (R_k + r)^2$, where E_k is the collision efficiency for the collector drop-smaller droplet pair. In a small distance δh, at any location, the probability of collision is a constant, equal to $\lambda_k \delta h$. We ignore the finite size effects which does not permit a collision at a distance less than the sum of radii of the collector drop and a smaller droplet. The probability of first collision in the δh neighborhood of h, which is $f(r|V_k)\delta r$, equals the product of the probability of no collision in the interval $(0, h)$, which is $G(r|V_k)$, and that of one collision in the interval $(h, h+\delta h)$, which is $\lambda_k \delta h$. We have assumed that the latter two events are statistically independent. Then $f(h|V_k)\delta h = G(h|V_k)\lambda_k \delta h$, and using Equation 1 we obtain the differential equation

$$-\frac{d}{dh} G(h|V_k) = G(h|V_k)\lambda_k \tag{3}$$

whose solution is $G(h|V_k) = \exp(-\lambda_k h)$. This implies that $f(h|V_k)$ is a Poisson distribution with the mean rate of collision λ_k. Hence the unclustered distribution of droplets is said to obey Poisson statistics at all scales (Shaw et al., 2002) or that the collision is a Poisson process. Equivalently the waiting time between consecutive collisions is exponentially distributed. This is modified in the presence of turbulence; for the second stage of growth Bec et al. (2016) showed that the waiting time between collisions changes to a Weibull distribution. Their result does not apply to the last stage of growth because the motion of the settling collector drops is not influenced by the background turbulence and hence is uncorrelated with the motion of the smaller droplets.

If there is clustering then inside a cluster the mean collision rate of the collector drop is enhanced, since a cluster has an above-average concentration of smaller droplets. For the same reason, when the collector drop suffers a collision it is more probable to be inside a cluster. Put another way, if the collector drop suffers a collision at some location, then the probability of suffering another collision a distance h away is enhanced to $\lambda_k(1+\eta(h))\delta h$, where $\eta(h)$ is a correlation function which measures the "memory" or "history-dependence" of the collector drop that has entered a cluster. In fact, this enhancement in the collision rate may be considered as the operational definition of "droplet clustering". Going over the same argument as before, we obtain in this general case:

$$\begin{aligned} -\frac{d}{dh} G(h|V_k) &= G(h|V_k)\lambda_k(1+\eta(h)) \\ G(h|V_k) &= \exp\left\{-\int_0^h dh' \lambda_k (1+\eta(h'))\right\} \end{aligned} \tag{4}$$

Droplet clusters are dynamic structures which are continuously rearranged by the in-cloud turbulence. Therefore from the collector drop's perspective, the droplet clusters are associated with a correlation length L, such that for distances of fall $h \gg L$ subsequent to a collision $\eta(h) \to 0$, that is, the collector drop samples an unclustered distribution over large distances of fall after a collision. We adopt a simple model in which the droplet clusters are characterized by two parameters: the enhancement in the collision rate $\delta\lambda$ inside the cluster (which relates to the excess droplet concentration there) and the correlation length L of the cluster as seen by the settling collector drop. We assume that the correlation decays exponentially:

$$\eta(h) = \frac{\delta\lambda}{\lambda_k} e^{-h/L} \tag{5}$$

Above equation says that, subsequent to a collision, the collector drop of radius R_k begins with an enhanced collision rate $\lambda_k + \delta\lambda$, which then exponentially decays to λ_k as $h/L \to \infty$. With the above expression for $\eta(r)$ we obtain the no-collision probability function in terms of dimensionless variables:

$$G(h^*|V_k) = \exp\left\{-\lambda_k^* h^* - C\left(1 - e^{-Kh^*}\right)\right\}, \tag{6}$$
$$h^* \equiv \lambda_0 h,\ \lambda_k^* \equiv \frac{\lambda_k}{\lambda_0},\ C \equiv \delta\lambda L,\ K \equiv (\lambda_0 L)^{-1}$$

Since λ_0 is the mean collision rate of the collector drop initially, λ_0^{-1} is a measure of the "mean free path" of the settling collector drop. h^* is therefore the distance of fall of the collector drop measured in the units of its mean free path. K is the ratio of the mean free path of the collector drop to the correlation length of the clusters. The dimensionless parameter C is salient because it quantifies the significance of clustering in relation to the collisional growth of a settling drop. Substituting $C = 0$ in Equation 6 we recover $G(h^*|V_k)$ for the unclustered case. Now substituting $t = -C\exp(-Kh^*)$ in the Laplace transform integral of $G(h^*|V_k)$, we obtain after simplification:

$$\mathbf{G}_k(s) = \mathbf{L}[G(h^*|V_k)] = \frac{(-C)^{-(s+\lambda_k^*)/K} e^{-C}}{K}\ \gamma\left(\frac{s+\lambda_k^*}{K}, -C\right) \tag{7}$$

where $\gamma(z,a) \equiv \int_0^a t^{z-1}e^{-t}dt$ is the lower incomplete gamma function (Arfken and Weber, 2005). $\mathbf{G}_k(s)$ from Equation 7 is inserted into Equation 2 and our task now is to find the inverse Laplace transform of the resulting expression. The inversion can be done in closed form as an infinite sum, see Appendix A; however the infinite sum converges too slowly to be of practical use. Therefore we shall evaluate the inverse Laplace transform numerically to obtain the results in this article. In the rest of the article we adopt the simplifying approximation that the collision efficiency remains constant as the collector drop grows, which implies:

$$\lambda_k^* = \frac{\lambda_k}{\lambda_0} = \frac{(R_k/r+1)^2}{(R_0/r+1)^2},\ \frac{R_k}{d} = \left(\left(\frac{R_0}{r}\right)^3 + k\right)^{1/3} \tag{8}$$

which is independent of both the collision efficiency E_c and the concentration of the smaller droplets n_0. Then $P(k|h^*, V_0)$ is also independent of E_c and n_0 (they appear only in the scale for h). The relevant dimensionless

parameters are then $h^*, R_0/r, k, K, C$.

We end this section by comparing the model proposed here with that due to Kostinski and Shaw (2005) and Telford (1955). Kostinski and Shaw (2005) modeled the collisions suffered by the settling collector drop as a Poisson process, in which the (stochastic) time between consecutive collisions is distributed exponentially. They also accounted for the change in the collision rate due to the changing collector drop size. Telford (1955) also made identical assumptions regarding the collision process, but while he solved a simplified stochastic collection equation to obtain the size distribution curve for the collector drops and then looked at the tail probabilities, Kostinski and Shaw (2005) showed that a simple, intuitive argument can be employed if one were to focus on the tail probabilities from the outset (they also showed how the size distribution curves can be obtained by analyzing the distribution of time between consecutive coalescences). In this article we too obtain the entire size distribution curve albeit with a cutoff at the drizzle drop size (see Section 4). Our model also accounts for the change in the collision efficiency with the changing collector drop size (Madival, 2018). However when there is clustering ($C > 0$) the distribution of time between consecutive collisions deviates from the exponential distribution. Probability functions f and G have been given in terms of the distance of fall h, but we can interpret them in terms of the time of fall by reinterpreting h^* as dimensionless time and λ_k as the mean collision rate per unit time (Madival, 2018). Then the first-collision probability function, f, also gives the distribution of the time between consecutive collisions; its dimensionless form is

$$f(h^*|V_k) = -\frac{d}{dh^*}G(h^*|V_k) = (\lambda_k^* + CKe^{-Kh^*})\ \exp\left\{-\lambda_k^* h^* - C\left(1 - e^{-Kh^*}\right)\right\} \tag{9}$$

which reduces to the exponential distribution when there is no clustering ($C = 0$).

3 | NUMERICS

While several methods are available in the literature for evaluating the inverse Laplace transform numerically, we employ Talbot (1979)'s method in the computationally efficient form developed by Abate and Valkó (2004). In Talbot's method, the contour of integration for the Bromwich integral in the complex s-plane (which gives the inverse Laplace transform explicitly, Arfken and Weber (2005)) is deformed so that on the deformed contour the oscillatory part of the complex-valued integrand is zero and hence the integral converges rapidly. To improve upon the earlier algorithms which were constrained by fixed machine-precision evaluation, Abate and Valkó exploited the multi-precision capability of symbolic computing tools such as Mathematica. They demonstrated the robustness of their algorithm by using it to invert several standard functions. In our case, the inverse transform is available in closed form for the unclustered distribution. The same is used here to test Abate and Valkó's algorithm. For an unclustered distribution of smaller droplets, $G(h^*|V_k) = \exp(-\lambda_k^* h^*)$, therefore $\mathbf{G}_k(s) = (s + \lambda_k^*)^{-1}$. This is inserted into Equation 2 and the resulting expression inverted to obtain the formula for the probability for k collision-and-coalescences in the unclustered case (Madival, 2018; Telford, 1955):

$$P(k|h^*, V_0) = \alpha \sum_{j=0}^{k} \frac{e^{-\lambda_j^* h^*}}{\beta_j}, \quad \alpha \equiv \prod_{i=0}^{k-1} \lambda_i^*,\ \beta_j \equiv \prod_{i=0,\ i\neq j}^{k} \left(\lambda_i^* - \lambda_j^*\right),\ h^* \equiv \lambda_0 h, \lambda_i^* \equiv \frac{\lambda_i}{\lambda_0} \tag{10}$$

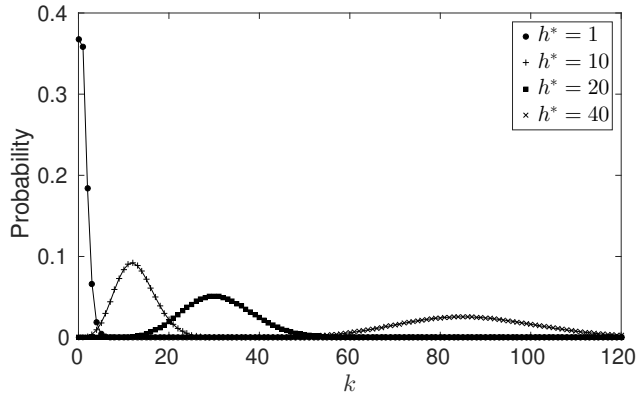

FIGURE 1 Numerically evaluated inverse Laplace transform using the algorithm of Abate and Valkó (2004) (discrete markers) compared to the exact formula Equation 10 (solid lines), for an unclustered distribution of smaller droplets for different values of h^*; $R_0 = 40$ μm, $r = 20$ μm.

We use the symbolic computing tool Mathematica for all the computations in this article. In Figure 1 we compare the numerically inverted Laplace transform using Abate and Valkó's algorithm with the exact formula Equation 10, for $R_0 = 40$ μm and $r = 20$ μm. The agreement between the numerics and the exact formula is excellent, with a maximum relative error of about 10^{-15}. Only the probability at $h^* = 0$ cannot be evaluated numerically, but this case is trivial: $P(k|h^* = 0, V_0)$ equals 1 for $k = 0$ and is zero for $k > 0$, because no collision can happen over zero distance of fall. Abate and Valkó's algorithm has one free parameter: number of terms M in the summation approximating the integral. The cost of computation for a specified accuracy, that is the required M, increases as k increases or as r approaches zero. In this article the computed probabilities did not change to 1 part in 10^6 for $M \geq 90$ and we have used $M = 100$ throughout. Further, as C is reduced the size distribution of the collector drops approaches that for the unclustered case; for $C = 10^{-2}$ the size distribution is practically identical to that for the unclustered case, see Figure 2. This further validates Abate and Valkó's algorithm as applied to the clustered case.

4 | RESULTS AND DISCUSSION

We consider collector drops of initial radius $R_0 = 40$ μm as appropriate for the last stage of growth (Grabowski and Wang, 2013) settling amidst smaller droplets of radii $r = 20$ μm and 15 μm (separately); to become drizzle (~ 100 μm radius) the collector drops must undergo 120 and 280 collision-and-coalescences respectively in the two cases. Decreasing the size of the smaller droplets requires more collisions for drizzle formation, which is computationally expensive. Fortunately the final results are insensitive to the variation of the size of the smaller droplets. Thus the only parameters of significance are K and C. Recall that K^{-1} is a dimensionless measure of the cluster size as perceived by the settling collector drop. C, the product of the enhancement in the collision rate inside a cluster and its size, is a more complete measure of the clustering. Figure 2 and ?? show the typical effect of increasing C on the collector drop growth (for $K = 100$, the largest K considered in this article); the probability curves are in fact the collector-drop size distributions (with drop volume being a measure of size) because k collision-and-coalescences imply a collector drop of volume $V_0 + kv$. For $C = 0.01$

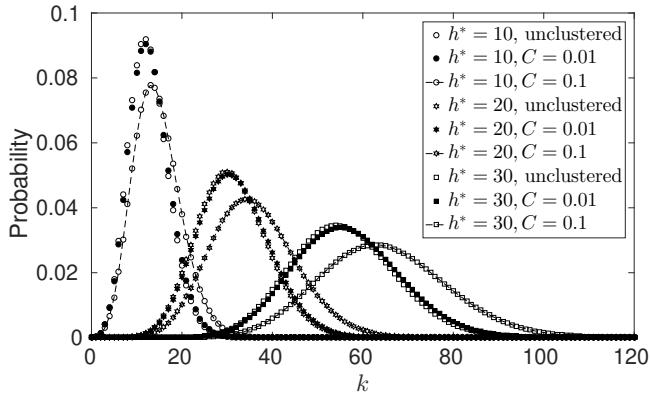

FIGURE 2 Effect of clustering on collector drop growth for different distances of fall h^*; $K = 100$, $R_0 = 40$ μm, $r = 20$ μm.

(Figure 2) the collector-drop size distribution for the clustered and the unclustered cases evolve at nearly the same pace, while for $C = 0.1$ the size distribution for the clustered case leads that for the unclustered case, signaling an increased growth rate of the settling collector drops due to clustering. Plotting Figure 2 on a log-linear scale reveals that, to a good approximation, the portion of the curves beyond the peak is exponentially decaying. The magnitude of K and C relevant to the clouds will be discussed later.

Summing the probabilities corresponding to any collector-drop size distribution curve in Figure 2 ("area under the curve") gives the fraction of the collector drops which have not yet become drizzle drops. In this article, drizzle is presumed to be initiated if 10% of the collector drops exceed 100 μm radius, that is when the area under the size distribution curve has decreased to 90%. For drizzle initiation, the required distance of fall in the clustered case, H^*, will be less than that in the unclustered case, H_u^*. Then $100 \times (1 - H^*/H_u^*)$ gives the percent reduction in the distance of fall needed to initiate drizzle, which is a robust measure of the enhancement in the collector drop growth due to clustering.

Figure 3 for $r = 20$ μm and Figure 4 for $r = 15$ μm show the reduction in the distance of fall required for drizzle initiation for $0.5 \leq K \leq 100$ and $0.1 \leq C \leq 10$. The qualitative shape of the curves may be anticipated; as clustering weakens, that is as $C \to 0$, the reduction in the distance of fall goes to zero, and as clustering becomes more intense, that is as $C \to \infty$, the reduction in the distance of fall asymptotes to 100%. For $K \geq 5$, the portion of the curve with $C \leq 2$ rises steeply; in this regime even a small increase in C leads to a significant enhancement in the collector drop growth. Most notably, Figure 3 and 4 are nearly identical with the ordinates of the corresponding data points differing by less than 2 in absolute magnitude. This shows that the reduction in the distance of fall due to clustering is rather insensitive to the choice of the smaller-droplet size.

We may also look at the growth in the time domain, that is we ask for the time needed (instead of the distance of fall) for initiation of drizzle. The two problems are not equivalent; since the settling velocity depends on the drop size, then depending on the individual history of collisions in a given duration of fall different collector drops will fall through different distances. We now need the settling velocity U_k of a collector drop as a function of its radius R_k. For the size range of interest to us we may assume that the settling velocity is proportional to the collector drop size (Rogers and Yau, 1996). For a collector drop of radius R_k, the mean

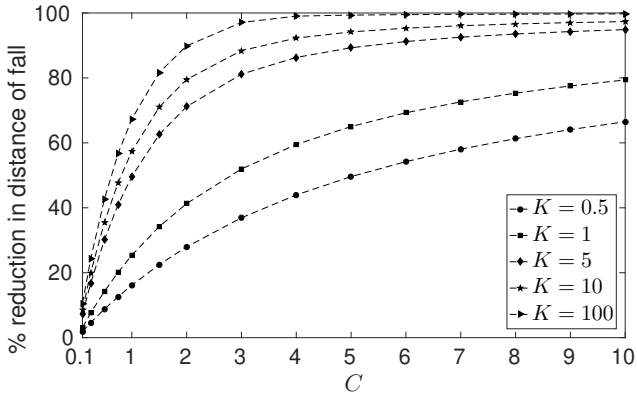

FIGURE 3 Percent reduction in distance of fall in the presence of clustering for 10% of 40 μm collector drops to become drizzle drops while settling amidst 20 μm drops. Broken lines are only to guide the eye.

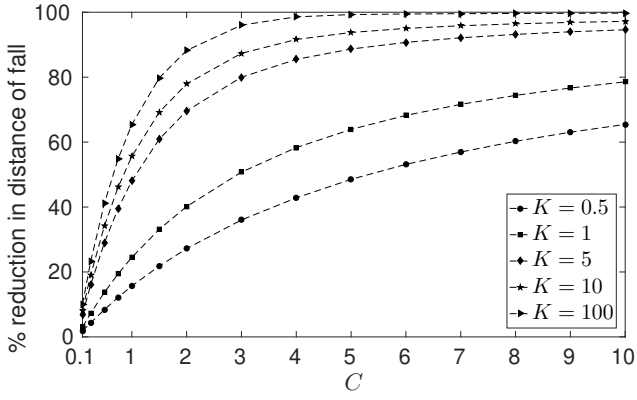

FIGURE 4 Percent reduction in distance of fall in the presence of clustering for 10% of 40 μm collector drops to become drizzle drops while settling amidst 15 μm drops. Broken lines are only to guide the eye.

number of collision-and-coalescences per unit time is $\tilde{\lambda}_k = U_k \lambda_k$, hence $\tilde{\lambda}_k^* = \tilde{\lambda}_k / \tilde{\lambda}_0 = (R_k/R_0)\lambda_k$. Defining the dimensionless time $t^* = \tilde{\lambda}_0 t$, we get the equations in the time domain by replacing h^* by t^* and λ_k^* by $\tilde{\lambda}_k^*$ in Equation 6, 7, 10, and 12 (Madival, 2018). The definition and physical interpretation of C and K remain the same. The reduction in time of fall for drizzle initiation due to clustering is shown in Figure 5 for $r = 20$ μm. As before the result for $r = 15$ μm differs negligibly from this and is not shown. However comparing Figure 5 (reduction in the time of fall) with Figure 3 (reduction in the distance of fall) we see that although the shape of the corresponding curves are qualitatively similar, for small K or large C the ordinate values of the corresponding data points slowly diverge from each other. For $K = 0.5$ the ordinates of the corresponding data points can differ by as much as 23 in absolute magnitude, while for $K = 100$ the difference throughout is less than 3. As before for $K \geq 5$ the portion of the curves with $C \leq 2$ rises steeply; in this regime even a small increase in C causes a significant enhancement of the collector drop growth.

What range of values for K and C are pertinent to the clouds? The data from the cloud traverse

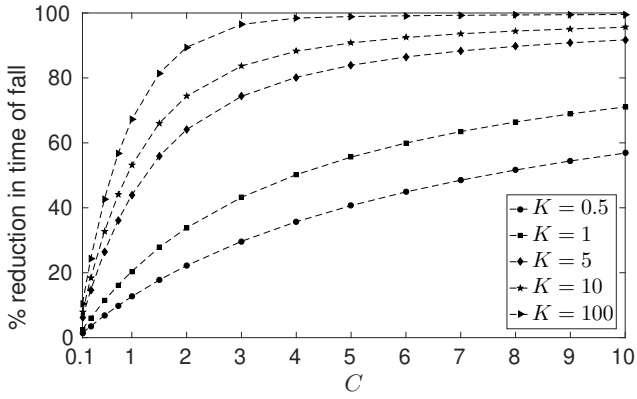

FIGURE 5 Percent reduction in time of fall in the presence of clustering for 10% of 40 μm collector drops to become drizzle drops while settling amidst 20 μm drops. Broken lines are only to guide the eye.

experiments do not always suffice to fix their values unambiguously and we must argue as to what is reasonable. We begin with $K^{-1} \equiv \lambda_0 L$, a dimensionless measure of the correlation-length or cluster-size L as perceived by the settling collector drop. In a clustered distribution of smaller droplets at a given instant, the clusters will be characterized by an instantaneous length scale L'. If the clusters are characterized by multiple length scales (for example, a "scale-free" distribution over a finite but large size range) then L' may be taken to be the largest among them. Numerical studies show that the inertial particle clustering can span from the dissipation scale to the inertial scale of turbulence (Bec et al., 2007; Yoshimoto and Goto, 2007). In-cloud turbulence has an inertial subrange spanning hundreds of meters (Shaw, 2003) which may be considered the maximum possible value for L'. However L' is an instantaneous quantity and is distinct from the correlation length L of clustering perceived by the settling collector drop. L can differ from the instantaneous quantity L' because the distribution of smaller droplets is continuously rearranged by the in-cloud turbulence. This is in fact the origin of the decaying memory effect incorporated into the probability functions f and G. If the settling speed U of the collector drop is small enough that the in-cloud turbulence is able to rearrange the distribution of the smaller droplets before the collector drop has fallen through the distance L' then $L < L'$. In fact we will assume $L \ll L'$, to be justified a posteriori. More intense the turbulence, smaller is the time needed to break up a cluster and rearrange the constituent droplets. The intensity of turbulence is measured by the production rate of turbulent kinetic energy, which for stationary turbulence equals the dissipation rate ϵ. Thus if L is primarily determined by the settling speed of the collector drop and the turbulence intensity then on dimensional grounds $L \sim U^3/\epsilon$. L depends on the collector drop size through U and some representative value of ϵ to be employed. For the 40 μm collector drop $U \approx 0.3$ m/s (Rogers and Yau, 1996) and for cumulus clouds $\epsilon \lesssim 10^{-1}$ m^{2}s^{-3} (Grabowski and Wang, 2013), hence L could be of the order of a meter as per our crude scaling argument. However this is likely an overestimate, since the most intense clustering is found to be at the dissipation scales, as revealed also by the recent in-cloud measurements (Larsen et al., 2018). Hence L cannot be far from the dissipation scale of the in-cloud turbulence. For the number density of smaller droplets $\sim$200 cc^{-1} (Shaw, 2003) we have $\lambda_0 \approx 1$; thus $K \gg 1$ is perhaps a conservative estimate for cumulus clouds. Improving this naive estimate demands an accurate model of the spatio-temporal evolution of droplet clusters in turbulence and is outside the scope of the present article. Note that as per our scaling argument K increases

with increasing turbulence intensity.

Next we estimate $C = \delta\lambda L = (\delta\lambda/\lambda_0)K^{-1}$ for the clouds. Recall that in Sect. 2, the function η of Equation 5 was introduced as a correction that modified the uniform probability of collision $\lambda_k \delta h$ for an unclustered distribution to $\lambda_k(1+\eta)\delta h$ for a clustered distribution. Such correction functions, called the "pair-correlation functions", have been reported in the studies of inertial particle clustering and in a few in-cloud measurements. The pair-correlation functions are instantaneous quantities and it is not clear if the correlation perceived by the settling collector drop over its finite duration of fall ought to conform to them. Nevertheless the magnitude of the instantaneous pair-correlation function at short distances from the collector drop must be nearly what it sees over that distance of fall. Larsen et al. (2018) found that at a distance of 1 mm the magnitude of the pair correlation function is $\sim 10^{-2}$, for clouds with dissipation rates $\sim 10^{-4} - 10^{-3}$ $\mathrm{m^2 s^{-3}}$. For shorter distances still we must rely on estimates from numerical studies based on simple model flows characterized by relatively low Reynolds number. Presence of gravity, along with polydispersity of drops, has been shown to reduce the spatial clustering of droplets (Rani et al., 2019a,b; Dhariwal and Bragg, 2018; Ireland et al., 2016b; Gustavsson et al., 2014; Zinchenko and Davis, 1994). From Ireland et al. (2016b), Dhariwal and Bragg (2018), which account for the effect of gravity on clustering, we assume that the maximum $\eta \sim 10$; from Equation 5, since $1 < \lambda_k/\lambda_0 \leq 2$, we have $\delta\lambda/\lambda_0 < 10$ and thus $C \leq 1$ for clouds. If $C \leq 0.1$ then the enhancement in the growth rate of the settling collector drops due to clustering is negligible.

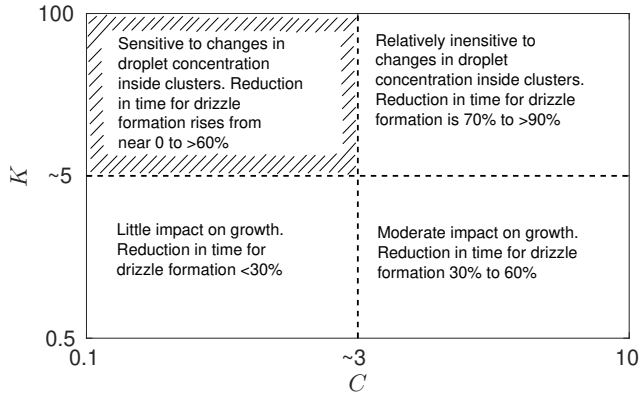

FIGURE 6 An approximate division of $K - C$ plane depending upon the reduction in time for drizzle formation in the last stage of growth. Hatched quadrant is probably where the clouds operate.

Based on our results the $K - C$ plane may be approximately divided into four quadrants, see Figure 6. In the lower left quadrant of low-K and low-C, the impact of clustering on the reduction in time for drizzle formation is rather negligible. On the other hand in the upper right quadrant of high-K and high-C the collector drop growth has saturated and there is little improvement in the reduction in time with increasing C. In the lower right quadrant of low-K and high-C the impact of clustering is substantial and the reduction in the time for drizzle formation can be $\sim 50\%$. However such high magnitudes of C are unrealistic as per our current understanding of the inertial particle clustering in the presence of gravity. In the upper left quadrant of high-K and low-C, the reduction in the time for drizzle formation is sensitive to changes in C (proportional to the excess droplet number concentration inside clusters) and this is presumably where the clouds operate.

In this regime even a small increase in clustering (increase in C) can significantly reduce the time for drizzle initiation. This is vindication of Telford (1955)'s insight that drizzle initiation is concerned with the evolution of tail probabilities of the droplet size distribution; hence large mean collision rates may not be needed to explain rapid drizzle formation, as many numerical and theoretical studies are wont to do in regard to the second stage of growth. Of course more in-cloud measurements are needed to identify the region of $K - C$ plane in which cumulus clouds operate. Finally, although the present study is aimed at the last stage of cloud drop growth, one may ask if the formalism here can be applied unchanged to the study of the second stage in which the collisional growth of cloud drops is primarily due to their interaction with the turbulence. Unfortunately we cannot, because in the second stage of growth two drops of even the same size can collide (Saffman and Turner, 1956) and thus the key assumption that there exists a population of collector drops that grow independently of each other breaks down.

5 | CONCLUSIONS

We studied the effect of clustering on the collisional growth of settling collector drops, as measured by the reduction in the time for drizzle initiation compared to the unclustered case. The effect of clustering on the collision process was incorporated by means of an exponentially decaying correlation function η in Equation 5 characterized by two parameters: increase in collision rate inside the cluster, $\delta\lambda$, and the correlation length L of the clusters as seen by the settling collector drops. They were encapsulated in dimensionless parameters $C = \delta\lambda L$ and $K = (\lambda_0 L)^{-1}$. Substantial reduction in the time needed for drizzle initiation is achieved for appropriate values of K and C, as displayed in Figure 5. Reduction in the time needed for drizzle initiation appears insensitive to the choice of smaller droplet size. Analysis based on several simplifying approximations showed that the cumulus clouds primarily operate in the range $K \gg 1$ and $C \leq 1$.. More significantly the present work identifies two simple parameters, K and C, that well characterize the effect of droplet clustering on the collisional growth of cloud droplets, at least for the last stage of cloud drop growth. We believe that delineating the region of the $K - C$ plane in which the clouds operate, by in-cloud measurements as well as in theory, is a fruitful avenue for future research.

ACKNOWLEDGEMENTS

The author thanks the anonymous reviewers for their insightful comments and suggestions, which has improved the quality of the manuscript considerably.

CONFLICT OF INTEREST

The author declares no conflict of interests in writing this article.

References

Abate, J. and Valkó, P. P. (2004) Multi–precision Laplace transform inversion. Int. J. Numer. Meth. Engng., 60, 979–993.

Alipchenkov, V. M. and Zaichik, L. I. (2003) Particle clustering in isotropic turbulent flow. Fluid Dynamics, 38, 417–432.

Arfken, G. B. and Weber, H. J. (2005) Mathematical methods for physicists. Elsevier India.

Ayala, O., Rosa, B., Wang, L. P. and Grabowski, W. W. (2008) Effects of turbulence on the geometric collision rate of sedimenting droplets. New J. Phys., 10, 075015.

Beard, K. V. and Ochs, H. T. (1984) Collection and coalescence efficiencies for accretion. J. Geophys. Res., 89, 7165–7169.

Bec, J., Biferale, L., Cencini, M., Lanotte, A., Musacchio, S. and Toschi, F. (2007) Heavy particle concentration in turbulence at dissipative and inertial scales. Phys. Rev. Lett., 98, 084502.

Bec, J., Celani, A., Cencini, M. and Musacchio, S. (2005) Clustering and collisions of heavy particles in random smooth flows. Phys. Fluids, 17, 073301.

Bec, J., Homann, H. and Ray, S. S. (2014) Gravity driven enhancement of heavy particle clustering in turbulent flow. Phys. Rev. Lett., 112, 184501.

Bec, J., Ray, S. S., Saw, E. W. and Homann, H. (2016) Abrupt growth of large aggregates by correlated coalescences in turbulent flow. Phys. Rev. E, 93, 031102.

Bender, C. M. and Orszag, S. A. (1999) Advanced Mathematical methods for scientists and engineers I. Springer-Verlag NewYork.

Bowen, E. G. (1950) The formation of rain by coalescence. Austral. J. Sci. Res. A, 3, 193–213.

Bragg, A. D., Ireland, P. J. and Collins, L. R. (2015) Mechanisms for the clustering of inertial particles in the inertial range of isotropic turbulence. Phys. Rev. E, 92, 023029.

Coleman, S. W. and Vassilicos, J. C. (2009) A unified sweep-stick mechanism to explain particle clustering in two and three dimensional homogeneous isotropic turbulence. Phys. Fluids, 21, 113301.

Davidson, P. A. (2007) Turbulence: An introduction for scientists and engineers. Oxford University press.

Devenish, B. J., Bartello, P., Brenguier, J. L., Collins, L. R., Grabowski, W. W., IJzermans, R. H., Malinowski, S. P., Reeks, M. W., Vassilicos, J. C., Wang, L. P. and Warhaft, Z. (2012) Droplet growth in warm turbulent clouds. Q. J. R. Meterol. Soc., 138(667), 1401–1429.

Dhariwal, R. and Bragg, A. D. (2018) Small–scale dynamics of settling, bidisperse particles in turbulence. J. Fluid Mech., 839, 594–620.

Eperin, T., Kleeorin, N., Krasovitov, B., Kulmala, M., Liberman, M., Rogachevskii, I. and Zilitinkevich, S. (2015) Acceleration of raindrop formation due to the tangling-clustering instability in a turbulent stratified atmosphere. Phys. Rev. E, 92, 013012.

Digital Library of Mathematical Functions (https://dlmf.nist.gov) National Institute of Standards and Technology, U.S. Department of Commerce. c. 2010-19, [Cited July 16, 2019]. Available from https://dlmf.nist.gov/8.11.

Grabowski, W. W. and Wang, L. P. (2013) Growth of cloud droplets in a turbulent environment. Annu. Rev. Fluid Mech., 45, 293–324.

Gualtieri, P., Picano, F., Sardina, G. and Casciola, C. M. (2013) Clustering and turbulence modulation in particle-laden shear flows. J. Fluid Mech., 715, 134–162.

Gustavsson, K. and Mehlig, B. (2016) Statistical models for spatial patterns of heavy particles in turbulence. Advances in Physics, 65, 1–57.

Gustavsson, K., Vajedi, S. and Mehlig, B. (2014) Clustering of particles falling in a turbulent flow. Phys. Rev. Lett., 112, 214501.

Ireland, P. J., Bragg, A. D. and Collins, L. R. (2016a) The effect of Reynolds number on inertial particle dynamics in isotropic turbulence. Part 1. Simulations without gravitational effects. J. Fluid Mech., 796, 617–658.

— (2016b) The effect of Reynolds number on inertial particle dynamics in isotropic turbulence. Part 2. Simulations with gravitational effects. J. Fluid Mech., 796, 659–711.

Jameson, A. R. and Kostinski, A. B. (2000) Fluctuation properties of precipitation. Part VI: Observations of hyperfine clustering and drop size distribution structures in three dimensional rain. J. Atmos. Sci., 57, 373–388.

Kostinski, A. B. and Jameson, A. R. (2003) On the spatial distribution of cloud particles. J. Atmos. Sci., 57, 901–915.

Kostinski, A. B. and Shaw, R. A. (2001) Scale dependent droplet clustering in turbulent clouds. J. Fluid Mech., 434, 389–398.

— (2005) Fluctuations and luck in droplet growth by coalescence. Bull. Am. Meteorol. Soc., 86, 235–244.

Langmuir, I. (1948) The production of rain by a chain reaction in cumulus clouds at temperatures above freezing. J. Meteor., 5, 175–192.

Larsen, M. L., Shaw, R. A., Kostinski, A. B. and Glienke, S. (2018) Fine–scale droplet clustering in atmospheric clouds: 3D radial distribution function from airborne digital holography. Phys. Rev. Lett., 121, 204501.

Lehmann, K., Siebert, H., Wendisch, M. and Shaw, R. A. (2007) Evidence for inertial droplet clustering in weakly turbulent clouds. Tellus B, 59, 57–65.

Madival, D. G. (2018) Stochastic growth of cloud droplets by collisions during settling. Theor. Comput. Fluid Dyn., 32, 235–244.

Maxey, M. R. (1987) The gravitational settling of aerosol particles in homogeneous turbulence and random flow fields. J. Fluid Mech., 174, 441–465.

Mehlig, B. and Wilkinson, M. (2004) Coagulation by random velocity fields as a Kramers problem. Phys. Rev. Lett., 92, 250602.

Narasimha, R. (2012) Cumulus clouds and convective boundary layers: A tropical perspective on two turbulent shear flows. J. Turbulence, 13(47), 1–25.

Pinsky, M. and Khain, A. (2003) Fine structure of cloud droplet concentration as seen from the fast-FSSP measurements. Part II: Results of in situ observations. J. Appl. Meteorol., 42, 65–73.

Pumir, A. and Wilkinson, M. (2016) Collisional aggregation due to turbulence. Annu. Rev. Condens. Matter Phys., 7, 141–170.

Rani, S. L., Dhariwal, R. and Koch, D. L. (2019a) Clustering of rapidly settling, low inertia particle pairs in isotropic turbulence. Part 2. Comparison of theory and DNS. J. Fluid Mech., 871, 450–476.

Rani, S. L., Gupta, V. K. and Koch, D. L. (2019b) Clustering of rapidly settling, low inertia particle pairs in isotropic turbulence. Part 1. Drift and diffusion flux closures. J. Fluid Mech., 871, 450–476.

Ray, B. and Collins, L. R. (2011) Preferential concentration and relative velocity statistics of inertial particles in navier-stokes turbulence with and without filtering. J. Fluid Mech., 680, 488–510.

Reade, W. C. and Collins, L. R. (2000) Effect of preferential concentration on turbulent collision rates. Phys. Fluids, 12, 2530–2540.

Rogers, R. R. and Yau, M. K. (1996) A short course in cloud physics. Butterworth-Heinemann.

Saffman, P. G. and Turner, J. S. (1956) On the collision of drops in turbulent clouds. J. Fluid Mech., 1, 16–30.

Saw, E. W., Shaw, R. A., Ayyalasomayajula, S., Chuang, P. Y. and Gylfason, A. (2008) Inertial clustering of particles in high Reynolds number turbulence. Phys. Rev. Lett., 100, 214501.

Shaw, R. A. (2003) Particle-turbulence interactions in atmospheric clouds. Annu. Rev. Fluid Mech., 35, 183–227.

Shaw, R. A., Kostinski, A. B. and Larsen, M. L. (2002) Towards quantifying droplet clustering in clouds. Q. J. R. Meterol. Soc., 128, 1043–1057.

Siebert, H., Gerashchenko, S., Gylfason, A., Lehmann, K. and Collins, L. R. (2010) Towards understanding the role of turbulence on droplets in clouds: In situ and laboratory mesurements. Atmos. Res., 97, 426–437.

Sundaram, S. and Collins, L. R. (1997) Collision statistics in an isotropic particle-laden turbulent suspension. Part 1. direct numerical simulations. J. Fluid Mech., 335, 75–109.

Vali, G., Kumowski, M. J., Rauber, R. M., Ochs, H. T. and Miller, L. J. (1997) The microphysical structure and evolution of Hawaiian rainband clouds. Part I: Radar observations of rainbands containing high reflectivity cores. J. Atmos. Sci., 54, 369–385.

Talbot, A. (1979) The accurate numerical inversion of Laplace transforms. J. Inst. Math. Appl, 23, 97–120.

Telford, J. W. (1955) A new aspect of coalescence theory. J. Meteorol., 12, 436–444.

Vohl, O., Mitra, S. K., Wurzler, S., Diehl, K. and Pruppacher, H. R. (2007) Collision efficiencies empirically determined from laboratory investigations of collisional growth of small raindrops in a laminar flow field. Atmos. Res., 85, 120–125.

Wang, L. P., Wexler, A. S. and Zhou, Y. (2000) Statistical mechanical description and modeling of turbulent collision of inertial particles. J. Fluid Mech., 415, 117–153.

Yoshimoto, H. and Goto, S. (2007) Self–similar clustering of inertial particles in homogeneous turbulence. J. Fluid Mech., 577, 275–286.

Zaichik, L. I., Simonin, O. and Alipchenkov, V. M. (2003) Two statistical models for predicting collision rates of inertial particles in homogeneous isotropic turbulence. Phys. Fluids, 15, 2995–3005.

Zhou, Y., Wexler, A. S. and Wang, L. P. (1998) On the collision rate of small particles in isotropic turbulence. II. Finite inertia case. Phys. Fluids, 10, 1206–1216.

Zinchenko, A. Z. and Davis, R. H. (1994) Gravity–induced coalescence of drops at arbitrary peclet numbers. J. Fluid Mech., 280, 119–148.

A | CLOSED FORM SOLUTION FOR THE CLUSTERED CASE

We must find

$$P(k|h^*, V_0) = \mathbf{L}^{-1}[\mathbf{P}_k(s)], \quad \mathbf{P}_k(s) \equiv \mathbf{G}_k(s) \prod_{i=0}^{k-1} \mathbf{f}_i(s)$$

where $\mathbf{G}_k(s)$ is given by Equation 7 and $\mathbf{f}_i(s) = 1 - s\mathbf{G}_i(s)$. We shall compute the inverse Laplace transform by evaluating the Bromwich integral (Arfken and Weber, 2005)

$$\mathbf{L}^{-1}[\mathbf{P}_k(s)] = \frac{1}{2\pi i}\int_Q ds\; e^{sh^*}\mathbf{P}_k(s)$$

where the path of integration Q is an infinite line parallel to the imaginary axis in the complex s-plane, chosen such that all the singularities of $\mathbf{P}_k(s)$ lie on the left of Q. The singularities of $\mathbf{P}_k(s)$ are that of the lower incomplete gamma function, $\gamma(z,a)$. The poles and residues of the lower incomplete gamma function are identical to that of the complete gamma function because the former is obtained by subtracting an analytic function from the latter. Therefore $\gamma(z,a)$ has a countably infinite number of simple poles on the negative real axis at $z = -n$ for $n \in \{0,1,2,\ldots\}$, with the corresponding residues $(-1)^n/n!$. The singularities of $\mathbf{P}_k(s)$ are therefore simple poles located on the negative real axis at $S_{j,n} = -\lambda_j^* - n\;K$, for $j \in \{0,1,\ldots,k\}$ and $n \in \{0,1,2,\ldots\}$. Thus Q may be chosen to be any vertical line in the complex s-plane that lies to the right of $s = -1$.

For fixed a we have $\gamma(z,a) \sim a^z e^{-a}\sum_{q=0}^{\infty}(a^q/(z)_{k+1})$ as $|z| \to \infty$, where $(z)_{k+1}$ is the falling factorial (Digital Library of Mathematical Functions, https://dlmf.nist.gov). In this limit $\mathbf{G}_k(s) \sim \sum_{q=0}^{\infty}(a^q/(z)_{k+1})$ where $a = -C$ and $z = (s+\lambda_k^*)/K$, and hence the integrand of the Bromwich integral above decays away from the origin in the left half of the complex s-plane. Thus the Bromwich integral under consideration is equal to the sum of the residues of its integrand at its simple poles:

$$\mathbf{L}^{-1}[\mathbf{P}_k(s)] = \sum_{j,n}\mathrm{Res}_{s=S_{j,n}}[e^{sh^*}\mathbf{P}_k(s)] = \sum_{j,n}\mathrm{Res}_{s=S_{j,n}}\left[e^{sh^*}\mathbf{G}_k(s)\prod_{i=0}^{k-1}\mathbf{f}_i(s)\right]$$

We assume that the poles of $\mathbf{G}_k(s)$ remain distinct, that is, if a and b are poles of $\mathbf{G}_i(s)$ and $\mathbf{G}_j(s)$ respectively then $a \neq b$ if $i \neq j$. Poles will be coincident if $(\lambda_i - \lambda_j)/K$ equals an integer for $i \neq j$, but Equation 8 shows this is unlikely for the most common cases. Therefore

$$\mathrm{Res}_{s=S_{j,n}}\left[\frac{1}{K}\Gamma\left(\frac{s+\lambda_k^*}{K}\right)\right] = \frac{(-1)^n}{n!}\delta_{jk}$$

where δ_{jk} is the Kronecker delta function. Using above result we obtain

$$\mathrm{Res}_{s=S_{j,n}}\left[\mathbf{G}_k(s)\right] = \frac{C^n e^{-C}}{n!}\delta_{jk},\;\; \mathrm{Res}_{s=S_{j,n}}\left[\mathbf{f}_k(s)\right] = -S_{j,n}\frac{C^n e^{-C}}{n!}\delta_{jk}$$

Thus the probability for k collision-and-coalescences of a collector drop that falls through a distance h^* among a clustered distribution of smaller droplets is:

$$P(k|r,V_0) = \sum_{n=0}^{\infty} \frac{C^n e^{-C}}{n!} \left\{ \sum_{j=0}^{k-1} -S_{j,n} e^{S_{j,n}h^*} \mathbf{G}_k(S_{j,n}) \prod_{i=0,\ i\neq j}^{k-1} \mathbf{f}_i(S_{k,n}) + e^{S_{k,n}h^*} \prod_{i=0}^{k-1} \mathbf{f}_i(S_{k,n}) \right\} \tag{11}$$

$$S_{j,n} = -\lambda_j^* - n\ K,\ h^* = \lambda_0 h,\ \lambda_k^* = \frac{\lambda_k}{\lambda_0},\ K = \frac{1}{\lambda_0 L},\ C = \delta\lambda L$$

$$\mathbf{G}_k(s) = \frac{(-C)^{-(s+\lambda_k^*)/K} e^{-C}}{K}\ \gamma\left(\frac{s+\lambda_k^*}{K}, -C\right),\ \mathbf{f}_i(s) = 1 - s\mathbf{G}_i(s)$$

To avoid ambiguity in the product notation we may also write the above result in the more explicit piecewise form:

$$P(k|r^*,V_0) = \begin{cases} \sum_{n=0}^{\infty} \frac{C^n e^{-C}}{n!} e^{S_{0,n}h^*} = e^{-h^* - C(1-e^{-Kh^*})} & , k=0 \\ \sum_{n=0}^{\infty} \frac{C^n e^{-C}}{n!} \left\{ -S_{0,n} e^{S_{0,n}h^*} \mathbf{G}_1(S_{0,n}) + e^{S_{1,n}h^*} \mathbf{f}_0(S_{1,n}) \right\} & , k=1 \\ \sum_{n=0}^{\infty} \frac{C^n e^{-C}}{n!} \left\{ \sum_{j=0}^{k-1} -S_{j,n} e^{S_{j,n}h^*} \mathbf{G}_k(S_{j,n}) \prod_{i=0,\ i\neq j}^{k-1} \mathbf{f}_i(S_{k,n}) + e^{S_{k,n}h^*} \prod_{i=0}^{k-1} \mathbf{f}_i(S_{k,n}) \right\} & , k \geq 2 \end{cases} \tag{12}$$

The case $k = 0$ is identical to $G(h^*|V_0)$ in Equation 6, as it should be. To recover the expression for the unclustered case, $P_{uc}(k|h^*, V_0)$, we take the limit $C \to 0$ of $P(k|h^*, V_0)$ in Equation 11. Only those terms corresponding to $n = 0$ survive. The symbolic computing tool Mathematica evaluates the limit $C \to 0$ of $\mathbf{G}_k(s)$ to be $(s + \lambda_k^*)^{-1}$. Since $S_{j,0} = -\lambda_j^*$ we obtain

$$P_{uc}(k|h^*,V_0) = \lim_{C\to 0} P_{uc}(k|h^*,V_0) = \sum_{j=0}^{k-1} \frac{\lambda_j^* e^{-\lambda_j^* h^*}}{-\lambda_j^* + \lambda_k^*} \prod_{i=0, i\neq j}^{k-1} \frac{\lambda_i^*}{-\lambda_j^* + \lambda_i^*} + e^{-\lambda_k^* h^*} \prod_{i=0}^{k-1} \frac{\lambda_i^*}{-\lambda_k^* + \lambda_i^*}$$

which after a slight rearrangement is seen to be identical to Equation 10, which therefore serves as a validation check.

We could not ascertain the domain of convergence of the infinite sum in Equation 12. If it converges at all then Equation 12 is to be implemented in a computer by replacing the infinite sum over n by $\sum_{n=0}^{n_{max}}$, where n_{max} is chosen such that the evaluated magnitude of $P(k|r^*, V_0)$ does not change (to specified accuracy) if we were to include terms beyond n_{max}. However the infinite sum converges too slowly (if at all) for this method to be practicable. Even with $n_{max} = 40$ which is already computationally intensive, we do not obtain satisfactory convergence, especially for large k. This is primarily due to those arguments of the lower incomplete gamma function lying close to its poles.